

Model refinement for the active control of thermoacoustic instability

Xiaochuan Yuan and Keith Glover

Abstract—Active control has been shown as a feasible technology for suppressing thermoacoustic instability in continuous combustion systems, and the control strategy design is substantially dependent on the reliability of the flame model. In this paper, refinement of G-equation flame model for the dynamics of lean premixed combustion is investigated. Precisely, the dynamics between the flame speed S_u and equivalence ratio ϕ are proposed based on numerical calculations and physical explanations. Finally, the developed model is tested on one set of experimental data.

I. NOMENCLATURE

ξ	flame position
S_u	flame surface velocity
ϕ	equivalence ratio
$\mathbf{u}(u, v)$	unburnt fluid velocity
ΔH	combustion enthalpy
η	combustion efficiency
ρ	fluid density
τ	convective time from the fuel injection point to the flame surface
$\bar{(\)}$	mean value
$(\)'$	perturbation in time domain
$\hat{(\)}$	perturbation in Laplace domain

II. INTRODUCTION

As lean premixed prevaporized (LPP) combustion technology is increasingly employed in the current combustor design for the purpose of reducing NO_x emissions, thermoacoustic instability has drawn particular attention since it is more likely to happen under lean combustion conditions. Reduced-order models have been proved effective in representing the fundamental properties of unsteady combustion oscillations and therefore serving as starting points for feedback control design. With the idea of extending the G-equation flame modeling approach for the lean premixed flames, a number of studies ([1], [2], [3], [4]) attempt to consider the impacts of perturbations in equivalence ratio on the combustion, a general method is to incorporate the empirical relationship between the flame speed S_u and equivalence ratio ϕ in the G-equation flame model.

However, this empirical equation taking the change of S_u as a function of ϕ is mostly derived from the fitting of lab-scale experimental data, which are measured under steady state conditions (see, e.g., [5]), thereby the dynamics between $S_u(t)$ and $\phi(t)$ has not been captured by this empirical function, and it can cause discrepancies between the results

from the reduced-order flame model and experimental data, particularly at high frequencies ([2]). The purpose of this paper is to make a proposition on the dynamics between $S_u(t)$ and $\phi(t)$ based on some combustion numerical calculations, moreover the dynamics assumption will be tested with experimental data.

In section III, the G-equation approach for flame modeling and how the empirical equation $S_u(\phi)$ merges into the reduced-order model are briefly introduced. Based on some fundamental knowledge in combustion calculation, section IV illustrates how the flame speed responses change as the frequency of the ϕ increase, thereby a first-order flame dynamics assumption is proposed. The flame models including the flame dynamics are tested on one set of experimental data in section IV-C.

III. G-EQUATION FLAME MODEL

By capturing the kinematic propagation of the flame front, the G-equation model provides an interpretation of how fluctuations in the inlet flow result in perturbations of the flame surface, thereby affecting the overall heat release. The model is based on the following assumptions:

- The flame is a thin surface separating the combustion products from the unburned mixture
- The flame moves at a velocity in a direction normal to its surface with speed S_u
- Compressibility effects and vorticity across the flame are not considered
- The structure of the flame surface is axisymmetric
- Pressure perturbations do not affect the flame surface structure
- The rate of the heat release is proportional to the instantaneous flame area

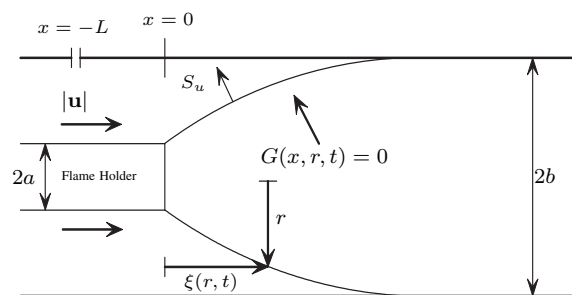


Fig. 1. Simple geometry of the setup in [6]

Take the combustion system in [6] as an example, its schematic is shown in Fig. 1. Suppose that combustion begins

X. Yuan is supported by Cambridge Overseas Trust

X. Yuan and K. Glover are with the faculty of the Department of Engineering, University of Cambridge, Trumpington Street, Cambridge CB2 1PZ, UK {xy240, kg103}

on a surface whose axial position is given by $x = \xi(r, t)$, so that $G(x, r, t) = 0$, where

$$G(x, r, t) = x - \xi(r, t) \quad (1)$$

And $G < 0$ for the unburned fluid with a velocity of $\mathbf{u}(u, v)$, where u and v denote the velocity components in the axial and radial direction respectively; While $G > 0$ for the products. The flame surface propagates according to the so-called G-equation:

$$\frac{\partial G}{\partial t} + \mathbf{u} \cdot \nabla G = S_u |\nabla G| \quad (2)$$

Substitute G in (2) with (1) gives:

$$\frac{\partial \xi}{\partial t} = u - v \frac{\partial \xi}{\partial r} - S_u \sqrt{1 + \left(\frac{\partial \xi}{\partial r}\right)^2} \quad (3)$$

Once the $\xi(r, t)$ is determined by solving the (3) with a specified oncoming velocity \mathbf{u} , the instantaneous heat release $Q(t)$ can be calculated by

$$Q(t) = \eta \rho_u S_u \Delta H \int_a^b 2\pi r \sqrt{1 + \left(\frac{\partial \xi}{\partial r}\right)^2} dr \quad (4)$$

The G-equation approach has been used to construct mathematical flame model for both premixed laminar flames ([7]) and turbulent flames ([6]).

IV. FLAME DYNAMICS

This section will aim to explain the issue of applying the empirical function $S_u(\phi)$ and propose a new assumption for the flame dynamics. A general form for the laminar flame speed is given as follows ([5]),

$$S_u(\phi) = k_1 \phi^{k_2} e^{-k_3(\phi - k_4)} \quad (5)$$

where k_i s are constants. The function of S_u in terms of ϕ is an empirical expression for the static relationship between S_u and ϕ . Flame speed S_u appears twice in the G-equation flame model, the first one comes into the PDEs (3) for the calculation of flame fronts position, the other one comes into the enthalpy calculation for the overall heat release integration in (4). Here we assume that the dynamics only come into the former one because of the following two reasons. Firstly, the two terms involve different combustion mechanism while the relationship between S_u and ϕ has been well studied, moreover, the investigation in [2] reveals the impact of fluctuations in ϕ at flame fronts PDEs (3) needs more inspection.

In the G-equation model ([6],[7], [1]) we assume the flame is simply a surface separating two thermodynamic states of unburnt and burnt gases related by overall mass and energy conservations, the mixing and combustion dynamics has not been considered. This assumption works very well for the laminar premixed flame, however, it is unrealistic for the turbulent premixed flame, which is the case in [1], [2].

The turbulent premixed flame in reality has a finite thickness, and the effects of fluctuating mixture will be different as the fluctuating frequencies change, at low frequencies as the wavelength of the fluctuation is much larger than the flame

surface thickness so that the flame can “see” the fluctuations, which would be more effective in changing the flame speed. However, when the frequency increases to the level that the wavelength of the fluctuation is comparable to the flame surface thickness, the flame will only “see” the mean value and the mixture fluctuation cannot take the same effects as it does at low frequencies.

Another important factor affecting the flame speed response is the diffusion in the combustion process. As the mixture travels from the fuel injection point to the flame fronts, its ingredient ratio will change as well, which leads to the variation of diffusion velocity along transportation. Based on some fundamental combustion knowledge, the rest of this section will try to present the impact of the equivalence ratio variation frequency on the flame speed response.

A. Problem formulation

It is known that strained premixed laminar can be viewed as being composed of a number of laminar flamelets. Structure and extinction of strained premixed flame have been extensively studied in order to apply the laminar flamelet concept to turbulent flame propagation (see, *e.g.*, [8]). The traditional analysis of strained flame is to reduce the governing equations to a boundary-value problem by invoking the boundary-layer assumptions together with stagnation point potential flow. In order to keep mathematical simplification, the setup in Figure 2 has been widely used ([9], [10]).

From an experimental viewpoint, these flames can be generated when a single reactant stream impinges on an adiabatic wall or when two counter-flowing reactant streams emerge from two counterflowing coaxial jets. When there is a single reactant jet, only one reaction zone is generated (see Figure 2(a)). However, if there are two reactant streams and each has the same exit velocity and equivalence ratio, then two flames symmetrical to the plane through the stagnation point are produced (see Figure 2(b)). The configuration has been extensively used in a number of theoretical and numerical studies (see, *e.g.*, [9], [10], [11]) of the premixed flames in a stagnation point flow. Here we choose methane (CH_4) as gas due to its simple chemical reaction mechanism and popular application in lab-scale combustion experiments.

The system is modeled by employing a boundary layer approximation, and the governing equations derived from continuity of mass, momentum, chemical species and energy can be written in the following forms [10],

$$\frac{\partial \rho u x^\alpha}{\partial x} + \frac{\partial \rho v x^\alpha}{\partial y} = 0 \quad (6a)$$

$$\rho u \frac{\partial u}{\partial x} + \rho v \frac{\partial u}{\partial y} + \frac{\partial p}{\partial x} = \frac{\partial}{\partial y} \left(\mu \frac{\partial u}{\partial y} \right) \quad (6b)$$

$$\rho u \frac{\partial Y_k}{\partial x} + \rho v \frac{\partial Y_k}{\partial y} + \frac{\partial}{\partial y} (\rho Y_k V_{ky}) - \dot{w}_k W_k = 0, \quad (6c)$$

$$k = 1, 2, \dots, K.$$

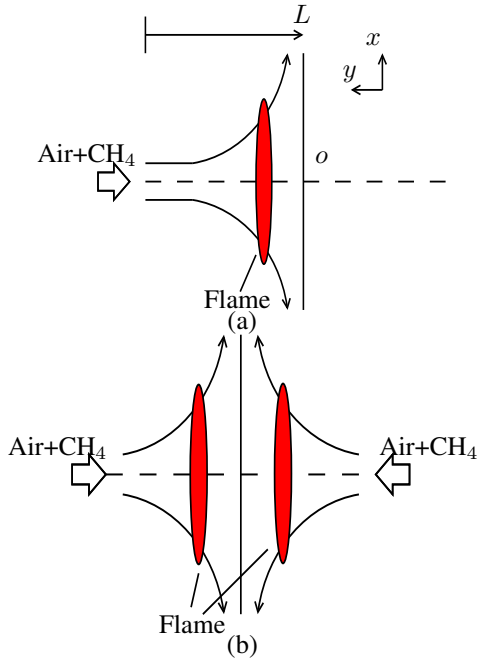


Fig. 2. Schematic of the stagnation point flow (a) single reactant stream configuration (b) counterflow configuration ([10])

$$\rho u c_p \frac{\partial T}{\partial x} + \rho v c_p \frac{\partial T}{\partial y} - \frac{\partial}{\partial y} \left(\lambda \frac{\partial T}{\partial y} \right) + \sum_{k=1}^K \rho Y_k V_{ky} c_{pk} \frac{\partial T}{\partial y} + \sum_{k=1}^K \dot{w}_k W_k h_k = 0 \quad (6d)$$

where α represents a geometric factor ($\alpha = 0$ for Cartesian coordinates and $\alpha = 1$ for cylindrical coordinates). In our case we set $\alpha = 0$ and suppose the gas satisfies the ideal gas law,

$$\rho = \frac{p\bar{W}}{RT} \quad (7)$$

Besides the common flow variables defined in the list of symbols, in these equations x and y denote the independent spatial coordinates (see Figure 2(a)), Y_k , the mass fraction of the k th species, u and v the velocity components of the incoming flow in the direction of x and y , respectively; W_k , the molecular weight of the mixture; λ , the thermal conductivity of the mixture; c_{pk} , the constant pressure heat capacity of the k th species; \dot{w}_k , the molar rate of production of the k th species per unit volume; h_k , the specific enthalpy of the k th species; μ , the viscosity of the mixture and V_{ky} , the diffusion velocity of the k th species in the y direction.

Numerous computational methods have been developed to find a solution for equations (6), which is not the major concern in our case. Here an advanced software tool COSILAB will be used to handle the complex numerical and chemical kinetics problems.

B. COSILAB

As a software tool for solving complex chemical kinetics problems, COSILAB¹ is widely used in industry and academia, particularly in automotive, combustion and chemical processing applications. It aims to solve problems involving thousands of reactions among hundreds of species for any mixture composition, pressure and temperature, and its computational capabilities enable a complex chemical reaction to be studied in detail, which includes intermediate compounds, trace compounds and pollutants.

Whilst complex chemistry is accounted for, chemical reactor or combustion geometries that can be handled by COSILAB are relatively simple, and this serves another reason for the application of the simple setup in Figure 2.

To investigate the effects of equivalence ratio variation on the methane-air laminar flames, an equivalence ratio oscillation is imposed at the boundary, and it follows a sine wave of frequency f and amplitude A_ϕ : $\phi = \phi_0 + A_\phi \sin(2\pi ft)$. The burner separation is taken as $L = 20\text{mm}$, the reactant composition are specified as mixture of methane and air (76.7% mass fraction of N_2 and 23.3% mass fraction of O_2). Steady solutions were obtained with the inlet velocity on the reactant side $|\bar{u}| = 1 \text{ m/s}$ and $\phi_0 = 0.75$.

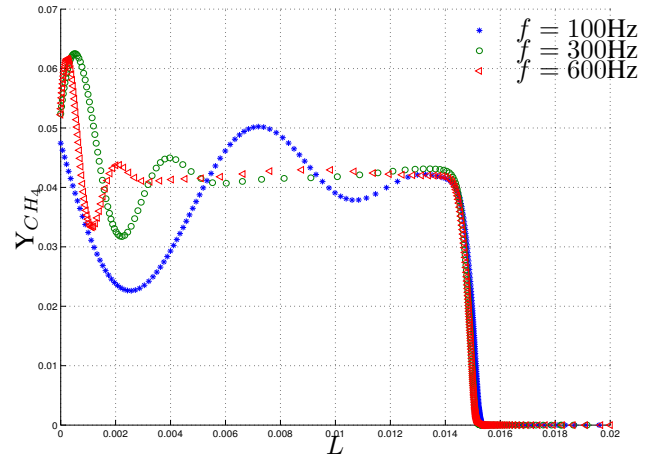


Fig. 3. Mass fraction of CH_4

To isolate the effect of frequency f in equivalence ratio fluctuations, the flow conditions for the flames studies herein have the same mean values and the imposed fluctuations of equivalence ratio have the same amplitude. In our case, $A_\phi = 0.5$ and $\phi_0 = 0.75$ in order to simulate the lean premixed flames, and three different frequencies $f = 100, 300, 600$ Hz with approximately five cycles simulation time are calculated. At the final time point, the mass fraction of CH_4 at the grid points on y -axis from 0 to L are shown in Fig. 3, the results show that the amplitude of the equivalence ratio oscillation will decay as the fluctuation convects towards the flame, thereby the amplitude “felt” by the flame is much less

¹<http://en.wikipedia.org/wiki/COSILAB>

than the amplitude A_ϕ at the boundary point. Further comparison of the results with different frequencies reveals that the amplitude of equivalence ratio oscillation decays towards the stagnation plane at a rate which increases with frequency. With perturbations in equivalence ratio convected towards the flame, its amplitude decreases because of diffusion. This results are consistent the conclusions in a number of studies, such as ([12], [13], [11]).

For the lean conditions studied here, the flame speed can be calculated by ([14], [11]),

$$S_u(x, t) = \frac{w_c}{\rho^u |\nabla c|} + \frac{\nabla \cdot (\rho D \nabla c)}{\rho^u |\nabla c|} + 2 \frac{\rho D \nabla Z \cdot \nabla c}{\rho^u |\nabla c| Z} \quad (8)$$

where the progress variables are defined as follows([14]),

$$c(x, t) = \frac{Y_{CH_4 0} Z(x, t) - Y_{CH_4}}{Y_{CH_4 0} Z(x, t) - Y_{CH_4}^{Eq} [Z(x, t)]} \quad (9)$$

with $Z(x, t)$ is the Bilger mixture fraction; $Y_{CH_4 0}$ is the fuel mass fraction in the fuel supply stream and $Y_{CH_4}^{Eq}$ is the equilibrium fuel mass fraction; ρ^u is the unburnt mixture density; $D(x, t)$ is the molecular diffusion coefficient.

By using the equations given in (8,9), the effects of the equivalence ratio variation on the flame speed response can be investigated numerically. Since that the amplitudes of equivalence ratio perturbations seen by the flame front are attenuated due to diffusion, the amplitudes of the resulting flame speed fluctuations will be attenuated as well. This has been confirmed in [11] which has computationally studied the effects of equivalence ratio variation on the flame structure and propagation. With different geometries and gases, the similar results have been obtained in a number of studies (see, *e.g.*, [12], [13], [11]).

C. Flame speed dynamics assumption

The simple numerical study in section IV-B, as well as a number of previous studies ([12], [13], [11]) have demonstrated that the amplitude of the flame speed response due to the equivalence ratio perturbation will decay at a rate which increase with frequency. One good physical description can be found in [12], which says that the flame's response is quasi-steady at low frequencies, while at higher frequencies the amplitudes of the induced oscillations are reduced and phase shifted with respect to the imposed signal. At still higher frequencies, the flame no longer responds to the oscillations in the external field.

Even though the conclusion is not novel in the field of combustion and flame, it has not be investigated in the reduced-order modeling for the lean premixed combustions. In the previous works ([1], [2], [3], [4]) attempting to incorporate the effects of equivalence ratio fluctuation in the G-equation flame model, such fluctuation is assumed to be transported unchanged towards the flame fronts, *i.e.*

$$\begin{cases} \phi(r, t) = \phi_0(t - \tau) \\ \phi_0 = \frac{|\bar{\mathbf{u}}| \bar{\phi}}{|\mathbf{u}|} \end{cases} \quad (10)$$

Then the flame speed S_u is calculated with (5).

Although it is extremely challenging to quantify the mixing and diffusion in the turbulent combustion process, based on the above numerical calculation for the simple setup in Fig. 2 and the above physical explanation, we make the following speculative assumption about the dynamics of \hat{S}_u ,

$$\hat{S}_u = \frac{K}{1 + T_s s} \frac{dS_u}{d\phi} \Big|_{\bar{\phi}} \hat{\phi} \quad (11)$$

where K and T_s are the DC gain and time constant respectively, and (11) will be used to represent the decreased high frequency gain caused by diffusion. The performance of the G-equation flame model with these two assumptions in (10) and (11) will be compared in the following section.

V. COMPARISON WITH EXPERIMENTAL RESULTS

In this section, we will test the developed models by using the experimental data in [15]. A schematic of the experimental rig is shown in Fig. 4, the rig is composed of a long circular duct of internal diameter 35 mm with a conical bluff body of diameter 25 mm. The flame is enclosed in a quartz cylinder with internal diameter 70 mm. The details of the experiments are omitted here for brevity and can be found in [15], [16].

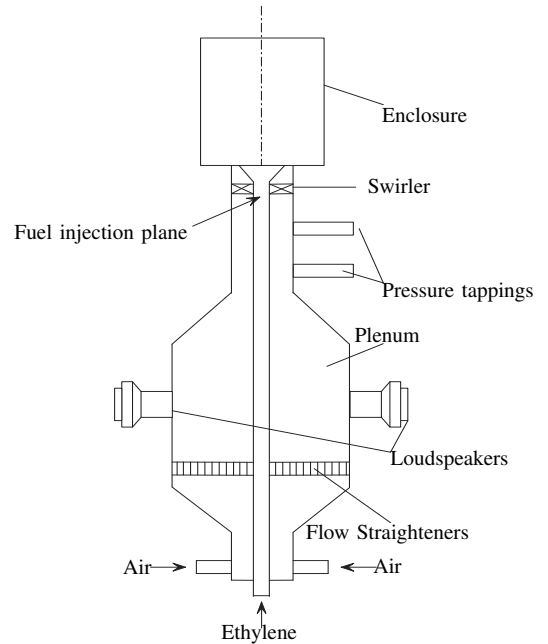


Fig. 4. Schematic of the burner used for the experiment in [15], [16]

To produce an enforced oscillation at the incoming flow, two loudspeakers are mounted diametrically opposite each other at about 1m upstream of the bluff body. The frequencies at which the velocity forcing was greatest was at 40 Hz and 160 Hz, and experimental measurements for imperfectly premixed combustion are available at these two frequencies. The heat release response are measured using OH^* and CH^* chemiluminescence.

The enforced incoming flow follows a sine wave of frequency f and amplitude A : $|\mathbf{u}| = |\bar{\mathbf{u}}|(1 + A \sin 2\pi f)$. We now proceed to calculate the simulation results using the model in [1] and make a comparison with the experimental results, the details of the reduced-order flame model can be found in [1], [2]. By referring to the results in [2], three cases are calculated with the parameters listed as follows,

- (1) Flame model with assumption in (10)
- (2) G-equation flame model with assumption in (11) ($K = 1, T_s = 1/300$)
- (3) G-equation flame model with assumption in (11) ($K = 0.5, T_s = 1/300$)

Comparing with the experimental results at 40 Hz and at 160 Hz, the plots in Fig. 5 show the amplitude of the perturbation in $Q(t)$ changes as function of forcing amplitude A . For Case (1), we see that there is a reasonable good agreement for 160 Hz, however, at 40 Hz there is a big gap between the simulation results and experimental data. With the flame dynamics assumption merged in the flame model, we can see obvious improvements in the model performance at both 40 and 160 Hz. In the experimental observations, at low forcing amplitudes, the flame response is linearly dependent on A . When the acoustic forcing amplitude increases, the flame surface will be increasingly curved and at some point the top part of the flame sheds from the main part. The abrupt change in the flame shape cause a sudden decrease in the flame fronts area, which in turn provide a “cap” on the amount of the overall heat release. Therefore, Fig. 5 implies that the simulation results from the flame model including assumption (11) provides better agreement with the experimental data.

The time series of the $\text{OH}^* \text{CH}^*$ measurements for various forcing amplitudes (used to obtain Fig. 5(a)) are presented in Fig. 6. The comparison in Fig. 6 suggests an evident improvement in the model performance after the flame dynamics has been included in the original flame model. It can be clearly seen that with increase in forcing amplitudes, the heat release measurements fluctuates nonlinearly and the increase in the heat release cycle is much steeper than its decay phase, at the bottom region of the heat release cycle will reach values very close to zero. Apart from a slight difference in phase and peak values, the model with flame dynamics assumption has successfully represented the features of the experimental results.

VI. CONCLUSION

For flame modeling in thermoacoustic instability control, the G-equation modeling approach is considered under the assumption that the flame is a thin surface separating the products from the unburnt mixture and moving at a constant velocity towards incoming flow. Without considering the dynamics between S_u and ϕ , the approach can somehow be extended for lean premixed combustion systems using the static equation between S_u of ϕ . We therefore provide evidence of issues inherent in using such empirical equation for lean premixed combustion modeling, moreover we make a proposition for the dynamics between S_u of ϕ based on

the some fundamental combustion knowledge as well as one basic numerical calculation about the flame speed. The model with such flame dynamics is tested with one set of experimental data and proved to be much more adequate in representing the experimental results.

To sum up, the proposed flame dynamics assumption significantly improves the performance of the lean premixed flame model. The resulting reduced-order flame model can be used not only for understanding the behavior of the combustion system, but also for construction of active control laws that would try to stabilize the unstable combustion oscillations.

VII. ACKNOWLEDGEMENTS

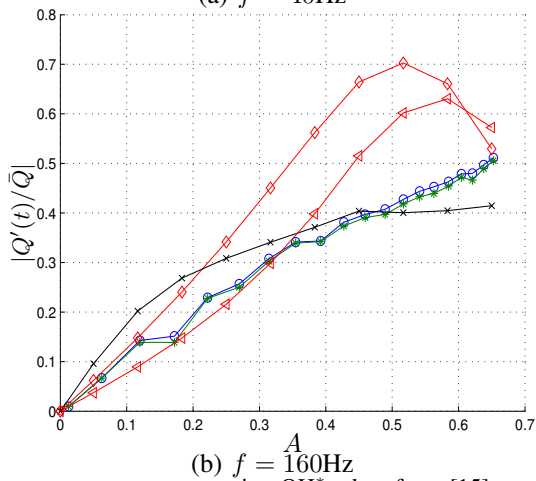
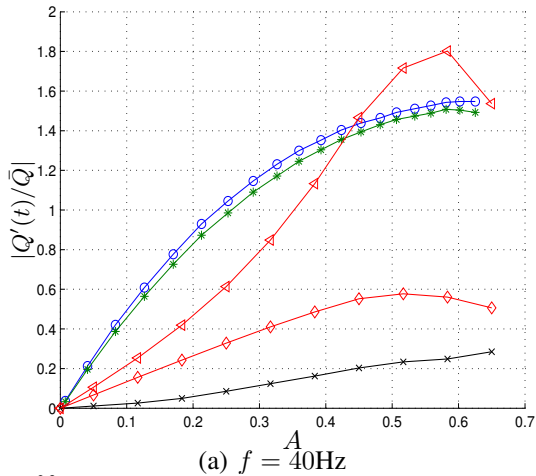
The authors would like to thank Dr Ramanarayanan Balachandran of University College London for providing the experimental data, Mr Ruigang Zhou of Cambridge Combustion Research Center for the fruitful discussions on the application of numerical combustion techniques.

REFERENCES

- [1] X. C. Yuan, K. Glover, and A. P. Dowling, “Modeling investigation for the thermoacoustic oscillation control,” in *Proceedings of 2010 American Control Conference*, 2010.
- [2] X. C. Yuan and K. Glover, “Model-based thermoacoustic oscillation control via \mathcal{H}_∞ loop-shaping and integral quadratic constraints,” in *Proceedings of 49th IEEE Conference on Decision and Control*, 2010.
- [3] A. P. Dowling and S. Hubbard, “Instability in lean premixed combustors,” *Proceedings of Institution of Mechanical Engineers*, vol. 214, no. 4, pp. 317–332, 2000.
- [4] S. Hubbard and A. P. Dowling, “Acoustic resonances of an industrial gas turbine combustion system,” *Transactions of the ASME*, vol. 123, pp. 766–773, 2001.
- [5] G. Abu-orf, “Laminar flamelet reaction rate modeling for spark ignition engines,” Ph.D. dissertation, University of Manchester Institute of Science and Technology, 1996.
- [6] A. P. Dowling, “A kinematic model of a ducted flame,” *Journal of Fluid Mechanics*, vol. 394, pp. 51–72, 1999.
- [7] M. Fleifil, A. M. Annaswamy, Z. Ghoniem, and A. F. G. and, “Response of a laminar premixed flame to flow oscillations: A kinematic model and thermoacoustic instability results,” *Combustion and Flame*, vol. 106, pp. 487–510, 1996.
- [8] P. A. Libby and K. N. C. Bray, “Implications of the laminar flamelet model in premixed turbulent combustion,” *Combustion and Flame*, vol. 39, pp. 33–41, 1980.
- [9] R. J. Kee, J. A. Miller, G. H. Evans, and G. Dixon-Lewis, “A computational model of the structure and extinction of strained, opposed flow, premixed methane-air flames,” *22nd Symposium (International) on Combustion/The Combustion Institute*, pp. 1479–1494, 1988.
- [10] V. Giovangigli and M. D. Smooke, “Extinction of strained premixed laminar flames with complex chemistry,” *Combustion science and technology*, vol. 53, pp. 23–49, 1987.
- [11] E. S. Richardson, V. E. Graneth, A. Eyssartier, and J. H. Chen, “Effects of equivalence ratio variation on lean, stratified methane-air laminar counterflow flames,” *Combustion Theory and Modelling*, 2010.
- [12] F. N. Egolfopoulos and C. S. Campbell, “Unsteady counterflowing strained diffusion flames: diffusion-limited frequency response,” *Journal of Fluid Mechanics*, vol. 318, pp. 1–29, 1996.
- [13] R. Lauvergne and F. N. Egolfopoulos, “Unsteady response of $\text{C}_3\text{H}_8/\text{air}$ laminar premixed flames submitted to mixture composition oscillations,” *Proceedings of Combustion Institute*, vol. 28, pp. 1841–1850, 2000.
- [14] K. Bray, P. Domingo, and L. Vervisch, “Role of the progress variable in models for partially premixed turbulent combustion,” *Combustion and Flame*, vol. 141, pp. 431–437, 2005.
- [15] R. Balachandran, “Experimental investigation of the response of turbulent premixed flames to acoustic oscillations,” Ph.D. dissertation, University of Cambridge, 2005.

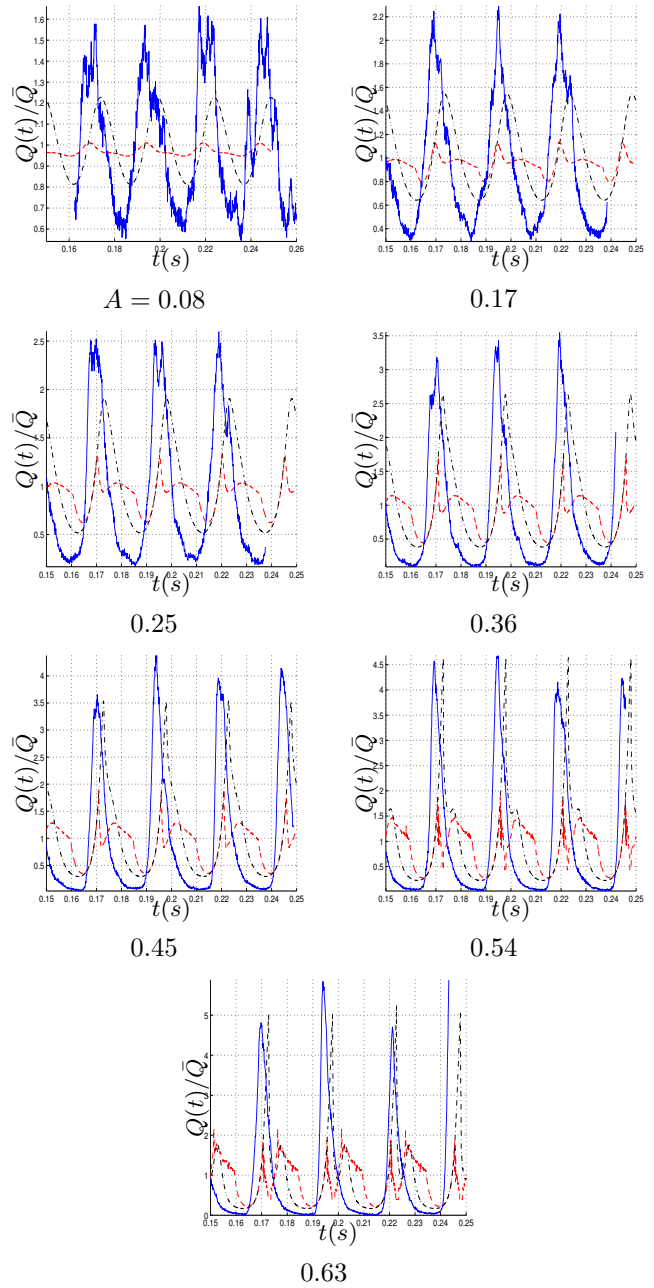
[16] R. Balachandran, B. O. Ayoola, C. F. Kaminski, A. P. Dowling, and E. Mastorakos, "Experimental investigation of the nonlinear response of turbulent premixed flames to imposed inlet velocity oscillations," *Combustion and Flame*, vol. 143, pp. 37–55, 2005.

APPENDIX



- —○—, measurements using OH* taken from [15]
- —*—, measurements using CH* taken from [15]
- —×—, Case (1)
- —◇—, Case (2)
- —△—, Case (3)

Fig. 5. The normalized global heat release fluctuation



- Experimental measurements taken from [15] (the solid line)
- Case (1) (the dashed line)
- Case (2) (the dash-dot line)

Fig. 6. Time series of heat release response from imperfectly premixed flame with different levels of forcing.